Environmental Technology & Innovation 25 (2022) 102150

Contents lists available at ScienceDirect

Environmental Technology & Innovation

journal homepage: www.elsevier.com/locate/eti

Recovery of iron nanominerals from sacred incense sticks ash waste collected from temples by wet and dry magnetic separation method

Nitin Gupta [a,1], Virendra Kumar Yadav [b,*,1], Krishna Kumar Yadav [d], Mamdooh Alwetaishi [e], G. Gnanamoorthy [f], Bijendra Singh [g], Byong-Hun Jeon [h], Marina M.S. Cabral-Pinto [i], Nisha Choudhary [c], Daoud Ali [j], Zahra Derakhshan Nejad [k]

[a] School of Nano Sciences, Central University of Gujarat, Gandhinagar, 382030, Gujarat, India
[b] Department of Microbiology, School of Sciences, P P Savani University, Kosamba, Surat, Gujarat, 394125, India
[c] Department of Environmental Science, School of Sciences, P P Savani University, Kosamba, Surat, Gujarat, 394125, India
[d] Faculty of Science and Technology, Madhyanchal Professional University, Ratibad, Bhopal, 462044, India
[e] Department of Civil Engineering, College of Engineering, Taif University, P.O. BOX 11099, Taif 21944, Saudi Arabia
[f] Department of Inorganic Chemistry, University of Madras, Guindy Campus Chennai 600025, Tamil Nadu, India
[g] School of Chemical Sciences, Central University of Gujarat, Gandhinagar, 382030, Gujarat, India
[h] Department of Earth Resources and Environmental Engineering, Hanyang University, Seoul 04763, Republic of Korea
[i] Geobiotec Research Centre, Department of Geoscience, University of Aveiro, 3810-193, Aveiro, Portugal
[j] Department of Zoology, College of Science, King Saud University, Riyadh, Saudi Arabia
[k] Department of Energy Resources and Geosystem Engineering, Sejong University, Seoul, Republic of Korea

ARTICLE INFO

Article history:
Received 5 June 2020
Received in revised form 2 October 2021
Accepted 19 November 2021
Available online 3 December 2021

Keywords:
Incense stick ash
Ferrous iron nanominerals
Hematite
Magnetite
Calcite

ABSTRACT

Indian incense stick ash (ISA) contains about 4%–8% ferrous iron (Fe^{2+}), the fourth-highest metal oxide mineral in ISA, as confirmed by X-ray fluorescence spectroscopy (XRF). The source of ferrous iron fractions in ISA is coal powder, which facilitates the burning of incense sticks. Ferrous iron is separated by two methods — dry and wet-slurry magnetic separation. Both are eco-friendly and cost-effective and assume a safe and rapid one-step process. The wet-slurry magnetic separation method is found to be more efficient, as its yield is almost twice the separation and purity level of the dry magnetic separation method. Various techniques have been employed to explore the chemical, physical, and morphological properties of recovered ferrous iron fractions. For example, Fourier transform-infrared spectroscopy (FTIR) and X-ray diffraction (XRD) have elucidated the micro-crystalline nature of the separated particles. Two types of microscopy techniques – field emission scanning electron microscopy (FESEM) and transmission electron microscopy (TEM) – have revealed the surface topography and morphology of the recovered ferrous iron particles, which are spherical and sized between 40 and 120 nm. Additionally, energy-dispersive X-ray spectroscopy (EDS) has confirmed that ferrous iron particles were rich in iron content, as the spectra showed prominent peaks for Fe and O, while the presence of Al, Si, Ca, Na, C, Na, Mg, Mn, and K indicates impurities associated with the samples.

* Corresponding author.
E-mail addresses: yadava94@gmail.com (V.K. Yadav), envirokrishna@gmail.com (K.K. Yadav).

[1] The authors contributed equally as the first author to this work.

https://doi.org/10.1016/j.eti.2021.102150

1. Introduction

In various civilizations, like those of ancient East Asia and the Middle East, incense sticks have been used in religious places to infuse the atmosphere with fresh air and eliminate bad energy (Lin et al., 2007). The typical composition of standard Indian incense sticks is 90%–95% sawdust, 4%–9% powdered charcoal, 0.1%–1% of an aroma-producing chemical, and the rest is a biomass binder enabling the rolling of the soft mass around a support wooden stick (Mukunda et al., 2007; Ramya et al., 2003). Burning incense sticks is a common practice in most South Asian countries, such as India, Pakistan, Taiwan, China, and Burma (Li et al., 2012; Bedini, 1963). In India, incense sticks are essential components of prayer in every house, without which worship is incomplete (Jetter et al., 2002). As a result, India is one of the largest producers and exporters and the second-largest consumer of incense sticks (after Taiwan) in the world (Hazarika et al., 2018; Jilla and Kura, 2017).

ISA is among the most uncharacterized by-products in houses and religious places. Every year, a million tons of incense sticks are burned around the globe, producing solid waste. In India, due to its holy values, ISA is disposed only into rivers (especially the Ganga) and other water bodies, such as lakes and oceans, which pollute India's natural water resources. In 1990, the National Council of Applied Economic Research (NCAER) and the National Group of Connected Financial Exploration (NGCFE) have performed a survey in India, estimating that a total of 147 billion incense stick ash was produced, with a cost of around 1.131 billion USD. In another study, it was determined that almost 60,000 million tons/annum of incense sticks were manufactured in India, which has an annual developing rate of 10%. Additionally, the All-India Agarbathi Manufacturers Association (AIAMA) has estimated the total export of incense sticks from India (Hanumappa, 1996). The report from 1989–90 shows that the total exports have been enhanced by ₹1.5 to ₹5 billion in the domestic market, which is around 266%. The trend continued in 2013, with the domestic market sales increasing to ₹ 36 billion, while the export to other countries attained ₹ 6 billion in 2013 with a compounded annual growth rate of 15% (AIAMA). Recently, the Indian incense sticks industry has estimated the rise in the sales of incense sticks in India. According to this estimation, incense sticks marketing increased from approximately ₹7.98 in 2015 to ₹9.65 billion in 2018 (Kumar, 2017).

ISA is hazardous and does not have any useful application to date. The typical composition of Indian ISA includes Ca, Si, Al, Mg, Fe, P, Na, and K (Yang et al., 2006). A similar composition was also reported by Khezri et al. (2015) from various types of ashes collected from Joss sticks after the Holy Ghost festival in Hungry. All these elements are present in their oxide form in large quantities. Out of these, Ca and Mg comprise about 50%–55% of the total ISA composition, and they are responsible for increasing the hardness of freshwater (Yadav et al., 2020). Moreover, both of these alkali metals, along with Na and K, are responsible for the increase of pH (alkalinity/basicity) in potable water (Kanchan et al., 2015), making this contaminated water unfit for drinking by altering its taste (Saha et al., 2019). The increased pH also affects the flora and fauna of impacted aquatic systems and, ultimately, harms the overall ecological system. Further, other alkali metals in the Indian ISA include Si, Al, and Fe, which are normally not toxic but may harm the aquatic systems in higher concentrations. Fe is an essential mineral, needed by plants and animals for normal growth and functioning (Gombart et al., 2020). However, an increase in Fe concentration may alter plants, small animals, and microbial diversity in the aquatic ecosystem. In addition to these elements, there is a high concentration of S and phosphorus oxides (10%–15%) (Elsayed et al., 2016), that, after disposal into water bodies, may form an acidic mixture and pose a threat to the living organisms within the affected aquatic system (Cabral-Pinto et al., 2020; See and Balasubramanian, 2011).

Indian incense sticks use coal powder as a facilitating agent for burning incense sticks. Coal contains various toxic heavy metals that remain in the ISA even after burning (Cui et al., 2019; Ali et al., 2019; Al-Ghouti et al., 2020; Quina et al., 2018). ISA is loaded with metals such as Hg, Cd, Mo, Ni, Pb, Cu, Cr, Zn, As, and Co (Frans va, 2009). ISA also comprises a mixture of various minerals such as calcite, silicates, periclase or magnesia, ferrous iron, and quartz (Lin et al., 2008). These versatile minerals are utilized in industries and other sectors, such as glass manufacturing, foundries, construction sites (concrete and masonry treatment), ceramics, and microchips (Jain et al., 2020). Detergent auxiliaries also use silicates in coating and industrial dyes. Additionally, silicate minerals are applied in the treatment of wastewater as an iron flocculent and alum coagulant (Sibiya et al., 2021; Tetteh and Rathilal, 2020). As mentioned previously, the disposal of ISA (loaded with toxic heavy metals) may pollute the water and pose a threat to all living organisms in aquatic systems. Moreover, these metals may be taken up by fish and lead to bioaccumulation, which may then enter the food chain following consumption by human beings (Venkateswarlu and Venkatrayulu, 2020). Once these heavy metals enter the human body, they may cause numerous maladies, such as neurological disorders, renal failure, carcinoma, and skin diseases (Vardhan et al., 2019; Gupta et al., 2019; Zierold et al., 2020). Therefore, it is necessary to focus on this potential problem and save clean drinking fresh water and the environment from ISA waste.

Two types of incense sticks are available on the Indian market, a black-coloured one, with coal or charcoal powder as a facilitating agent for burning, and a masala-based, light coloured one, which contains potassium nitrate as the facilitator for burning (Lin et al., 2008). It is shown that coal and its respective fly ashes contain ferrous, alumina, and silica with various toxic heavy metals (Zarenezhad et al., 2021). However, in the case of black-coloured incense sticks, approximately 10%–25% weight of incense sticks is made up of coal or charcoal powder. The average ferrous content in a black-coloured Indian ISA is about 5%–8%, which is the fourth-highest concentration of an element present in ISA, as confirmed by XRF (Table 1). The ferrous iron content may vary, based on the percentage of coal powder used for making incense paste (See and Balasubramanian, 2011), which varies across incense stick brands. It should be understood that Indian coal contains

Table 1
Elemental analysis of ISA residue obtained from, spot 1, spot 2, and spot 3 by EDS.

	Fe	K	O	C	Na	Mg	Al	Si	Ca
001	0.58	0.74	49.83	11.48	7.50	3.09	0.88	18.93	6.98
002	1.42	0.98	41.52	12.99	7.35	3.25	1.09	25.95	5.43
003	0.63	0.67	46.81	15.39	7.87	2.48		22.36	3.78
Average	0.88	0.80	46.05	13.29	7.57	2.94	0.99	22.41	5.40
SD	0.47	0.16	4.20	1.97	0.27	0.41	0.15	3.51	1.60

high amounts of Si, Al, and Fe in their oxide forms, which is why these are also present in ISA. The ferrous material in coal is present in the pyrite form, which gets transformed into ferrous oxides upon burning (Smołka-Danielowska et al., 2019). The temperature achieved during incense sticks burning is over 200 °C. At these temperatures, the pyrite transforms into a maghemite form of iron oxide (Mukunda et al., 2007; Gupta et al., 2019). Moreover, the ferrous particles in ISA are present, along with impurities such as Al, Si, Na, Ca, Mg, and carbon (Yadav et al., 2020). Such types of ferrous (Fe^{2+}) nanoparticles (Fe^{2+} NPs) are used as heterogeneous catalysts, adsorbents, and environmental clean-up materials. Further, (Fe^{2+} NPs) are utilized in ore processing, smelting, and steel production (Montoya-Bautista et al., 2019; Tavker et al., 2021).

The objective of the present research is two-fold: (a) the recovery of ferrous nanominerals (Fe-NMs) from ISA waste, using an economically and sustainably viable approach, and (b) the development of safe and sustainable management techniques for ISA waste. In our previous study, we have reported the synthesis of amorphous iron oxide particles from the recovered ferrous fractions of ISA. In this study, we have tried to observe the efficiency of the recovery of ferrous fractions by both dry and wet slurry magnetic separation techniques. The wet slurry-based separation provided more yield, which could be applied in industries for the recovery of ferrous fractions at an industrial scale. The recovered ferrous nanoparticles were thoroughly analysed for their chemical and elemental properties. Additionally, the analysis of final non-ferrous residues has revealed the non-separable ferrous present in ISA in a bound form. It is believed that the recovery of ferrous iron fractions from ISA will not only minimize the resultant solid waste but also reduce the water pollution resulting from the disposal of heavy metals and alkali metals from the ISA loaded into rivers. The present study was conducted in order to recover Fe-NMs from the ISA waste by using a safe, cost-effective, and sustainable method, which is also a pioneering one.

2. Materials and methods

2.1. Sample collection and apparatus

Incense sticks ash was collected from various temples of Gandhinagar, Gujarat, India. Glass beaker of 50–250 ml capacity (Borosil, India), double distilled water (DDW), Teflon-coated magnetic retriever rods (procured from Axiva, India), and circular (5 cm $\times$2 cm) strong neodymium magnet were procured from A–Z magnet, Chandni Chowk, Delhi, India.

2.2. Recovery of ferrous nanoparticle

Two methods of ferrous nanoparticle (Fe^{2+} NPs) separation that are the simplest, fastest, non-toxic (without using solvents, acids, or bases), and cost-effective are dry and wet separation methods. These protocols were used to recover the high-purity Fe-NMs from ISA waste through magnetic separation methods (Valeev et al., 2019; Malav et al., 2019). The ISA has 5%–8% ferrous content, confirmed by the XRF analysis (Horiba, model no. XGT-2700 X-ray). Ferrous particles were present freely and bounded internally with other minerals in the ISA.

The XRF analysis (Horiba, model no. XGT-2700 X-ray) revealed that 5%–8% ferrous was initially present in the ISA, which comprises separate ferrous oxide minerals and is internally bound to another mineral. The sample preparation and modelling of the instrument have already been reported by Yadav et al. (2021). Freely available ferrous in the form of ferrous fractions can only respond to an external magnet, which is why only those were recovered. While a small percentage of Fe were was internally bound with other minerals and did not respond to the external magnetic field, which is why it could not be collected, as they were firmly internally attached and weakly magnetized during the application of an external magnetic field (Lin et al., 2007).

2.2.1. Dry separation method

In the dry separation method, approximately 10 g of ISA waste were placed in a beaker. An external circular neodymium magnet was held in place with a magnetic retriever rod and directly introduced to the incense sticks ash and moved back and forth over it for 5–10 min. After the completion of this step, some of the Fe-NMs were adhered to the external surface of the neodymium magnet and detached manually by swiping with fingers into a glass Petri plate. Again the magnet was passed over the ISA, in back and forth direction, due to which some of the ferrous particles got adhered on the surface of magnet. Again, the adhered ferrous were detached manually, by using fingers or spatula. This step was repeated several times, till all adhere able ferrous particles were recovered from ISA. Finally, the collected Fe-NMs were weighed on the weighing balance and the value was noted down (Gupta and Yan, 2016).

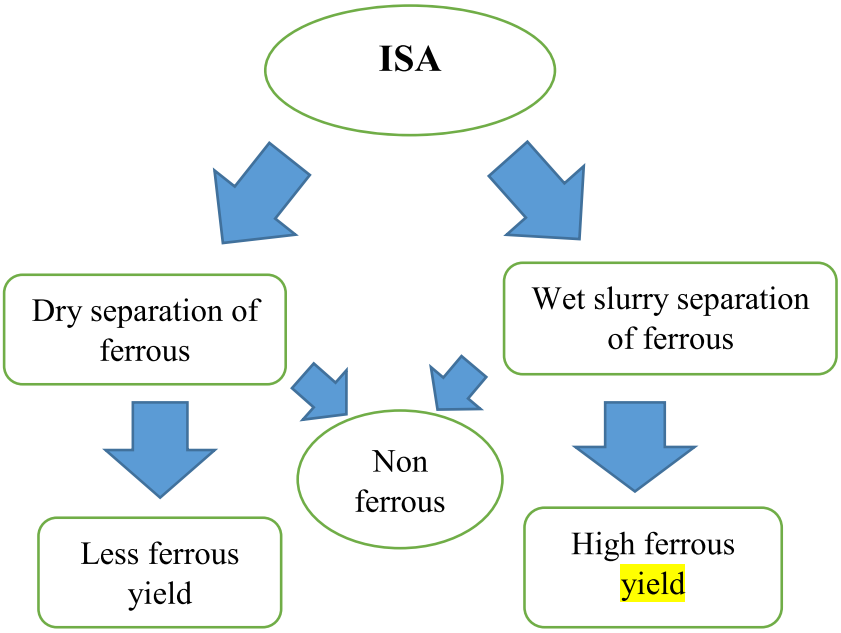

Fig. 1. Schematic diagram for extraction of Fe-NMs from ISA.

2.2.2. Wet-slurry separation method

In this method, approximately 10 g of ISA were placed in a beaker and 100 ml of double-distilled water (DDW) was added to form a slurry. The mixture was kept in a water bath ultrasonicator (Sonar 40 kHz) for 30 min at 50 ± 5 °C to break apart any aggregated particles so that trapped ferrous particles could get released. After 30 min, the neodymium magnet attached to the magnetic retriever rod (used in the dry separation method) was introduced directly into the slurry and stirred in clockwise and counter-clockwise directions. This step was repeated 3–4 times to ensure that all Fe-NMs have been recovered. The Fe-NMs on the surface of the magnet were separated manually by fingers and placed into a Petri plate. The recovered Fe-NMs were washed with DDW with pressure (from the wash bottle) by placing the magnet beneath the Fe-NMs. This step eliminated loosely bound non-ferrous fractions and aided the purification of recovered ferrous nanoparticles. Finally, the purified Fe-NMs were dried in a hot air oven at 50 ± 3 °C for 24 h. After drying, the recovered ferrous iron fraction was weighed carefully on the weighing balance and their value was noted down. Fig. 1 shows the schematic representation of the recovery of Fe-NMs from the ISA waste, while Fig. 2 exhibits separation of Fe-NMs by wet slurry method.

2.3. Characterization of recovered Fe-NMs

The Fe-NMs from ISA were analysed using various advanced microscopic and spectroscopic techniques. We applied Field Emission Scanning Electron Microscopy (FESEM) and High-Resolution Transmission Electron Microscopy (HR-TEM) to analyse the morphology (size, shape) and the surface topography of the Fe-NMs separated/recovered from the ISA waste.

The topography and structural properties were revealed through FESEM, NOVA NANOSEM-450, FEI, USA. The purified Fe-NMs were spread on a double-sided carbon tape, which was fixed to an aluminium stub. Gold sputtering was conducted for 10 min to make a charge-conductive particle. The morphology (size, shape) of the Fe-NMs was analysed by HRTEM, TECNAI 200 kV TEM (FEI, Electron Optics). For TEM analysis, 1 mg of Fe-NMs was added to the 40 ml DDW and dispersed by an ultrasonicator (Sonar, 40 kHz) for 5–10 min. A drop of dispersion medium was cast on carbon-coated copper grids and dried at room temperature before the grid was placed into the TEM.

FTIR analysis by (Perkin Elmer, Germany, SP 65) was conducted in order to identify functional groups on the Fe-NMs' surfaces. The analysis was performed using the KBr pellet technique, where 3mg of Fe-NMs were mixed with 197 mg of KBr. The solution was mixed with a mortar and pestle, making a thin pellet by a pellet maker. Scanning was done in the range of 4000 to 400 cm^{-1} with a spectral resolution of 1 nm in the transmittance mode. The hydrodynamic and particle size distribution of ferrous iron was carried out by dispersing the Fe-NMs in the DDW, followed by ultrasonication for 10 min to reach a uniform dispersion. The particle size was measured by a particle size analyzer (PSA) (Malvern Zetasizer Nano S90, UK) at 25 °C and a detection angle of 90°. The X-ray diffraction (XRD) analysis helped identify the phase and crystallinity of the Fe-NMs. The dry powder of Fe-NMs was scanned in the 2θ range of 10–80° on a Bruker,

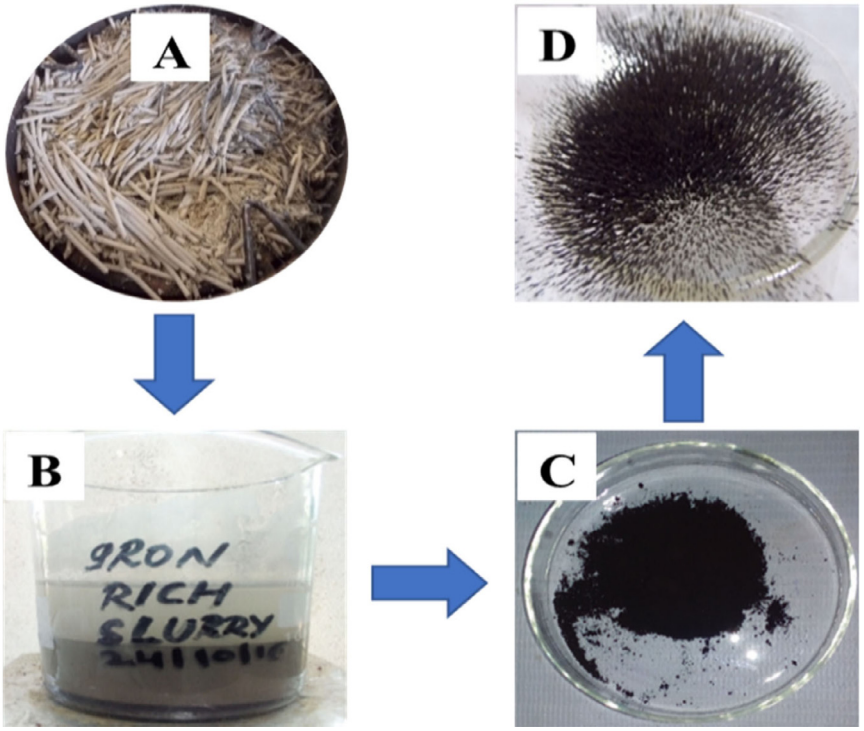

Fig. 2. Steps involved in the recovery of ferrous iron nanominerals (Fe-NMs) from ISA waste by using wet-slurry separation method (A) Collection of large amounts of ISA. (B) Preparation of Fe-NMs rich ISA slurry using tap water. (C) The separated-out Fe-NMs from the slurry of ISA waste using strong external neodymium magnet and washed from tap water to remove other heavy metals. (D) Dried and pure Fe-NMs.

D8 Advance diffractometer using a Cu-Kα radiation source. The elemental analysis was carried out by the Oxford-made energy-dispersive X-ray spectroscopy (EDS) detector attached to the FESEM instrument. The X-ray fluorescence (XRF) analysis was carried out using a Horiba model no. XGT-2700 X-ray analytical microscope, fitted with a high-purity silicon detector (XEROPHY) X-ray tube with Rh target. It was operated at a 40 kV X-ray tube (50 W). A solid pellet was prepared by mixing 5–8 g of ISA with sodium bromide (NaBr) powder in a mechanical presser machine (Perk Systems).

3. Results and discussion

3.1. Morphological and elemental analysis of ISA and ISA-residue

ISA is rich in Ca and carbon particles (Kao and Wang, 2002), which are highly aggregated together to form a lump as shown in the FESEM images of ISA in Fig. 3 A. The individual particles are micron-sized, i.e., 0.2–2 μm. Fig. 3B, shows the EDS spot of ISA, while Fig. 3C shows EDS spectra and elemental table of ISA. The EDS spectra clearly show that peaks for ISA are a mixture of numerous elements, which is evident from Fig. 3C, which shows peaks for C, Si, O, Ca, Fe, Na, K, Al, and Fe. Oxygen is present in the highest amount (41.7%), C (22.3%), Si (20%), Ca (5%), Na (4.3%), K (2%), Mg (1.8%), Al (1.8), and Fe (1.1%). The selected EDS spot was rich in silica, otherwise, Indian ISA have comparatively lesser amount of Si than the Ca. These elements are present in the form of oxides, as evident from a higher percentage of O in the ISA. Lin et al. (2007) reported that incense sticks and their ashes have a high content of Ca in the form of oxides and carbonates. Besides this, it also has a high amount of C and Mg, Na, Fe, Cu, Mn, and Zn, with wood as the source.

They reported a positive correlation between the total metallic content (TMC) and the ash emission factor, as well as a strongly positive correlation between the TMC and the burning rate. So, the burning rate of incense sticks is greatly influenced by the TMC. Similarly, Ca, Mg, K, Fe, and Al content have strong positive correlations with the burning rates of incense sticks, while no correlation was found between the burning rate and Na. Khezri et al. (2015) also reported that Ca was present in the highest amount, followed by Fe and Al, from the ashes collected from the Joss sticks during the Holy Ghost festival in Hungary.

Fig. 3D is a FESEM image which depicts 3, different EDS spots of ISA residue after the recovery of Fe-NMs by the wet separation method. The morphology of the ISA particles is almost intact, even after ferrous particles' separation. Fig. 3E–G shows the EDS spectra of different regions of ISA residue, although all elements in the ISA residue were almost the same as in the ISA, with only their concentration varying from region to region, as evident from EDS spots. Thus, it was found

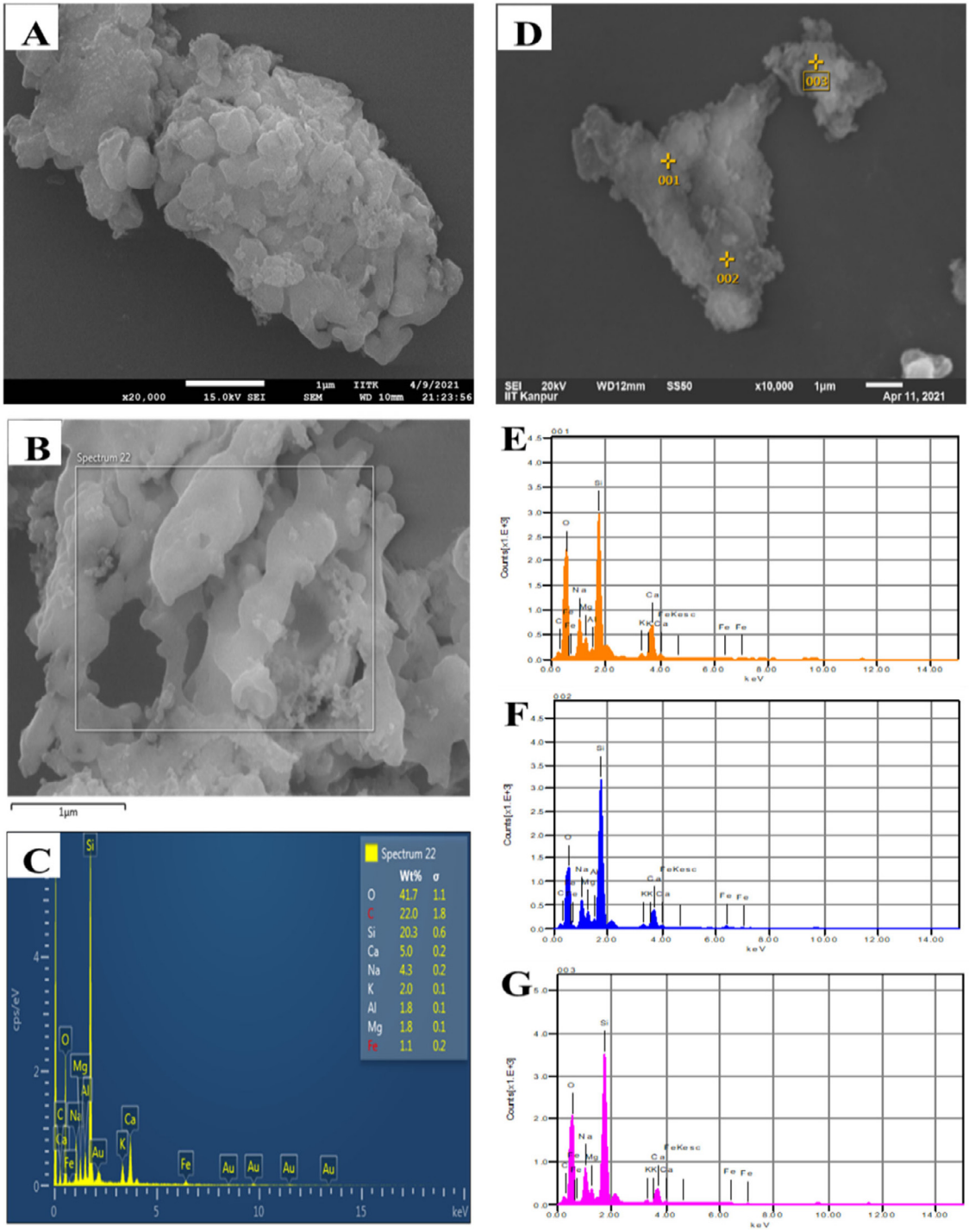

Fig. 3. (A) FESEM micrographs images of ISA at size scale (magnification) 1 µm (20,000x), (B) EDS spot of ISA (C) EDS spectrum and elemental table of ISA, (D) FESEM image depicting 3 different EDS spot of ISA residue, and (E, F, G) EDS spectra of ISA residue.

that the ISA and its residues are heterogeneous (Jain et al., 2020). Some of the elements got increased, while some of the elements got decreased after the recovery of ferrous particles from the ISA which is given in Table 1. The percentage of Fe, K, C, and Al decreased, while the value of the rest of the elements increased. So, the percentage of Fe decreased in the

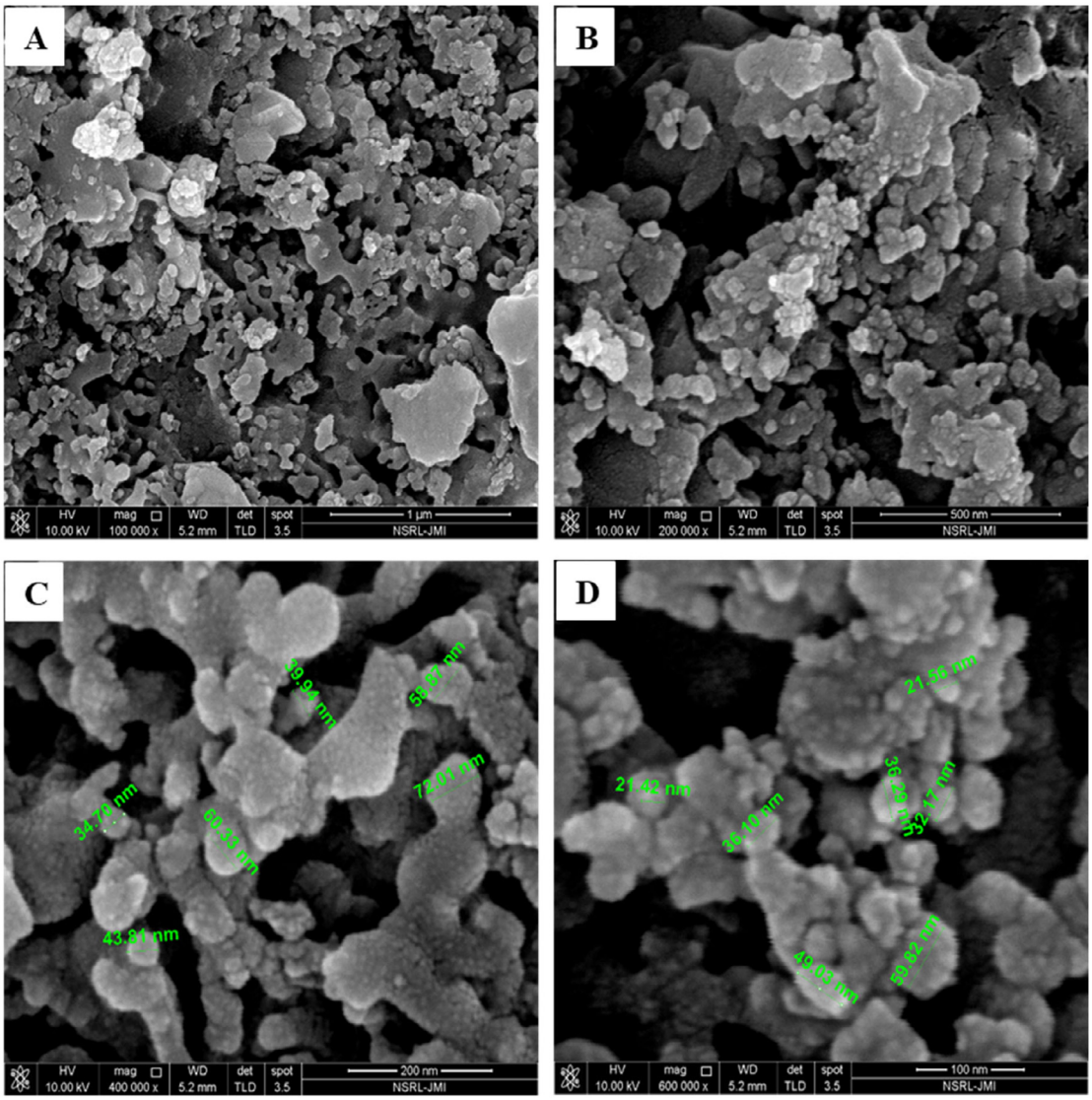

Fig. 4. FESEM micrographs of Fe-NMs separated from ISA at different size scales (magnifications), which are (A) 1 µm (100,000x), (B) 500 nm (200,000x), (C) 200 nm (400,000x), and (D) 100 nm (600,000x).

ISA residue, which confirms the recovery of ferrous particles from the ISA, which was about 15%–25% by applying wet magnetic separation.

3.2. Assessment of recovered Fe-NMs

Both separation methods were applied to recover Fe-NMs from the ISA and both were effective in separating sufficient quantities of Fe-NMs. In the dry separation method, around 2 g of Fe-NMs were recovered from 10 g of the ISA waste. The obtained Fe-NMs had a high level of impurities in the form of numerous non-magnetic fractions shown in Fig. 5B. However, with the wet separation method, approximately 4 g of Fe-NMs were separated from the same quantity of the ISA waste (10 g), which is twice the quantity separated with the previous method, with a high degree of purity due to the small quantity of non-magnetic fractions. Based on the analysis of separation methods, the wet-slurry separation method was found to be superior to the dry separation method for the recovery of Fe-NMs from the ISA waste. Moreover, the recovered Fe-NMs had a high level of purity as most of the non-magnetic fractions associated with the magnetic fractions were eliminated during washing. Therefore, we selected a wet-slurry method for the recovery of ferrous iron fractions from ISA for further research.

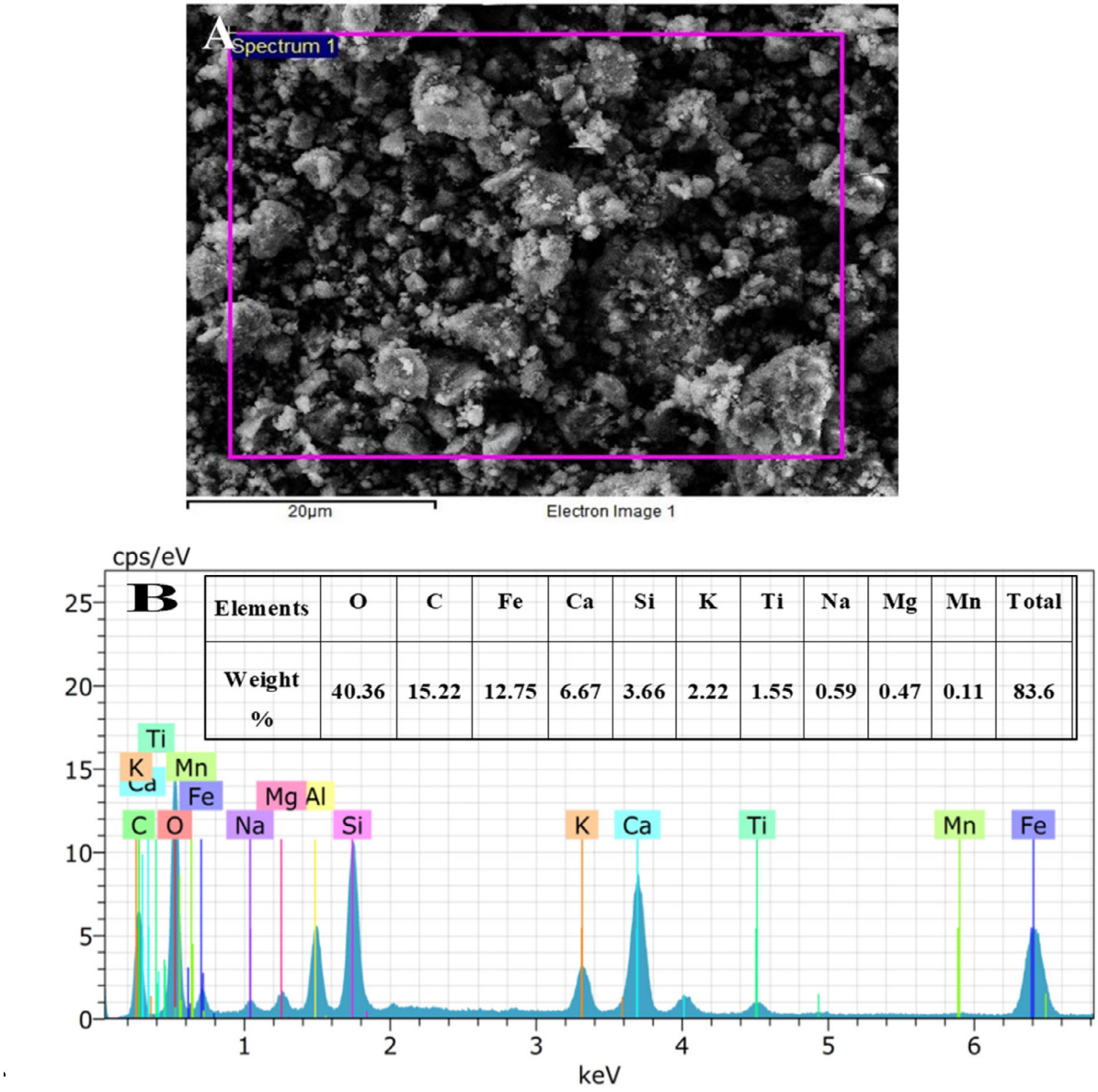

Fig. 5. EDS spot (A) and EDS spectrum and elemental table (B) of recovered Fe-NMs from ISA.

When one gram of ISA was dispersed in 10 ml of DDW, whose initial pH was 7.1, the pH level raised to 8.21. This indicates the change brought by the disposal of tonnes of ISA into the fresh river water or other water bodies. Such alkaline pH is harmful for the consumption and survival of aquatic flora and fauna.

3.3. Microscopic analysis

Fig. 4(A–D) depicts the FESEM micrographs of recovered Fe-NMs from the ISA waste at different size scales. The shape of most of the separated ferrous iron particles is irregular or spherical, and the nanoparticles were highly aggregated. Shapes or iron particles can be irregular due to the presence of unburnt carbon associated with the Fe^{2+} NPs. As the temperature during the incense sticks combustion is not very high, the ferrous particles (Fe^{2+}) failed to achieve any shape. The agglomeration could be due to the presence of a large amount of carbon in ISA, as incense sticks contain a large number of sources of carbon, such as bamboo, fragrance, essential oils, and coal powder, or sawdust (Ezhumalai et al., 2021).

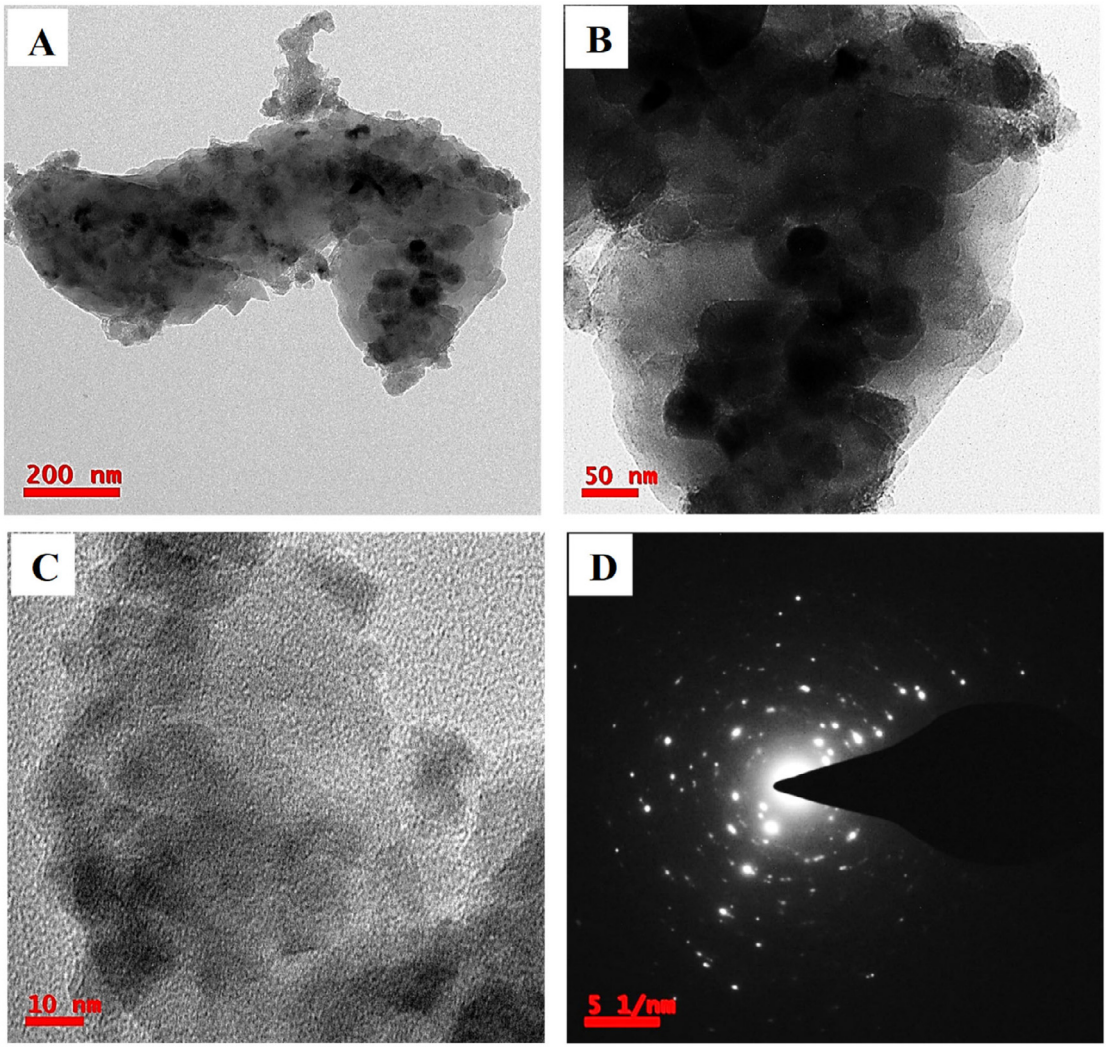

Fig. 6. TEM micrographs of Fe-NMs recovered from ISA waste at different size scales (A) 200 nm (B) 50 nm. (C) 10 nm. (D) SAED pattern of recovered Fe-NMs.

The EDS spectrum in Fig. 5B of the recovered Fe-NMs indicates the sharp peaks of Fe and O as major elements. There are other elements such as Al, Si, Mg, Na, Mn, Ca, K, P, Ti, and C, which are present as impurities, as shown in elemental table, Fig. 5B. The EDS spectrum indicates that Fe and O are always associated with Ca, C, O, and Si.

Carbon is present at about 15.22%, which is due to the organic nature of ISA. Higher compositions of carbon also indicate the presence of carbonates along with Fe-NMs. The carbon could also be present due to the unburned carbon, soot, chars, etc. in the separated Fe-NMs. Mn, Mg, and Na are present in traces in the smallest amounts in Fe-NMs. The presence of Ca, Si, Al, Mg, and Ti may be due to a higher composition of these elements in ISA. High content of calcium in the ISA was also reported by Lin et al. (2007), who investigated the emission products and metallic content after incense sticks burning. They also found a high content of alkali metals (Ca, Mg, Na), arguing that they were mainly used as enhancers in smoldering (Yeh et al., 1993). Such alkali metals could be applied to incomplete combustion (for example, incense) to cut down on air pollution.

The TEM images of Fe-NMs separated from ISA at two different size scales are shown in Fig. 6(A and B). Fig. 6(A and B) show the size scale of the micrograph at 200 nm and 50 nm, respectively. These images have dark black colour and light particles where the dark black particles are Fe-NPs and the light-coloured particles are electron-deficient particles, such as Ca and carbon. The black-coloured particles are mainly spherical and their size varies from 40 to 120 nm. Further, Fig. 6C shows HRTEM images of the ferrous iron-rich particles at the size scale of 10 nm, and Fig. 6D displays the selected area electron diffraction (SAED) pattern of the Fe-NMs, which indicates that the Fe-NMs are polycrystalline in nature.

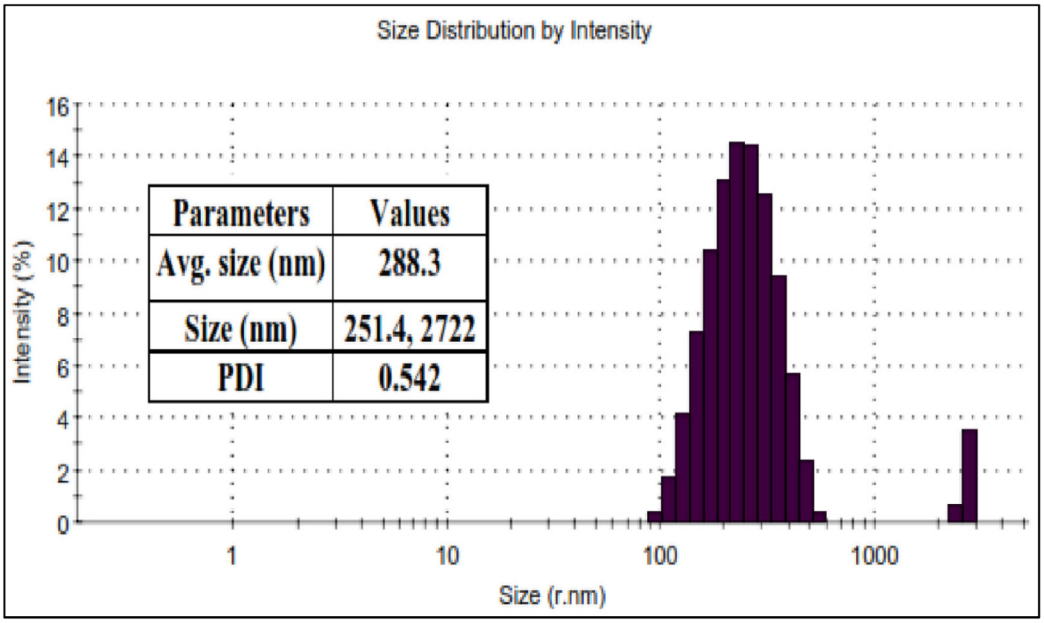

Fig. 7. Digital image of the particle size distribution of separated Fe-NMs from ISA waste.

Table 2
Major FTIR assignments in the Fe-NMs separated from ISA.

Minerals	Asymmetric stretching vibrations of C–O/Si–O–Si	Symmetric stretching vibrations of CO_3^{2-}	External plane bending vibrations of CO_3^{2-}/Fe–O	Internal plane bending vibrations of O–C–O	Stretching vibrations of Fe–O
Calcium carbonate	1422	1018	872	718	–
Ferrous iron	1422	–	872	718	522
Silicates/quartz	–	1018	–	–	–

3.4. Spectroscopic analysis

Fig. 7 displays the particle size distribution of ISA separated Fe^{2+}-NPs. The particles were dispersed in distilled water and sonicated for 10 min in an ultrasonicator before analysis. The sample was run twice to obtain the average size of the ferrous iron particles, which was 288.3 nm with a polydispersity index of 0.542.

Two types of particles present in the samples were sized at 251.4 nm and 2.722 μ. The size revealed by PSA is much greater than the FESEM analyses, which could be because dry samples were used for FESEM analysis while PSA used the hydrodynamic radius for its analysis in a liquid. Hence, the size analysed by PSA is bigger than the microscopic techniques. Similar results were also obtained by Yadav et al. (2021), where the iron oxide particles were synthesized from the ferrous particles recovered from ISA. The size reported by PSA was comparatively bigger than the average size reported by PSA.

Fig. 8 A depicts a typical full range (4000–400 cm^{-1} on X-axis) FTIR spectrum of Fe-NMs separated from ISA. Fig. 6B shows the enlarged spectrum of the same at a range from 1600 to 400 cm^{-1} on the *X*-axis. The spectrum exhibits several sharp and broad absorption peaks. The absorption peaks at 872, 718, and 522 cm^{-1} are characteristic signature peaks of iron oxides, which are attributed to the Fe–O bond (Khan et al., 2021). These bonds occur due to the symmetric, asymmetric, bending, and rocking vibrations of the Fe–O bonds. The peak at 1018 cm^{-1} is associated with the Si–O–Si bonds of silicates or quartz associated with the Fe-NMs from the coal powder (Khale and Chaudhary, 2007). This indicates the presence of quartz with ferrous iron particles. The peaks at 872 and 718 cm^{-1} could also be due to the external plane bending vibrations of carbonates and the internal plane bending vibrations of O–C–O of carbonates, respectively (Alavi and Morsali, 2010; Biradar et al., 2011; Li et al., 2013; Salavati-Niasari et al., 2015). The band at 1422 cm^{-1} corresponded to the asymmetric vibrations of the C—O bond in the carbonate, which confirms the association of calcium carbonates along with ferrous iron material as an important impurity, which was further confirmed by other spectroscopic techniques, such as EDS and XRD. Besides this, there are no impurities associated with Fe-NMs. Table 2 shows the absorption peaks and their relevant functional groups observed in the separated Fe-NMs from ISA.

A typical XRD diffractogram of ISA and ferrous iron particles is shown in Fig. 8(C and D). Fig. 8C exhibits a typical full-range XRD diffractogram, while Fig. 8D shows an enlarged diffractogram of the same. The XRD peaks indicate major mineral phases and crystallinity of the ISA. The XRD pattern reveals strong intensity peaks at 38.46° and 44.49°, which

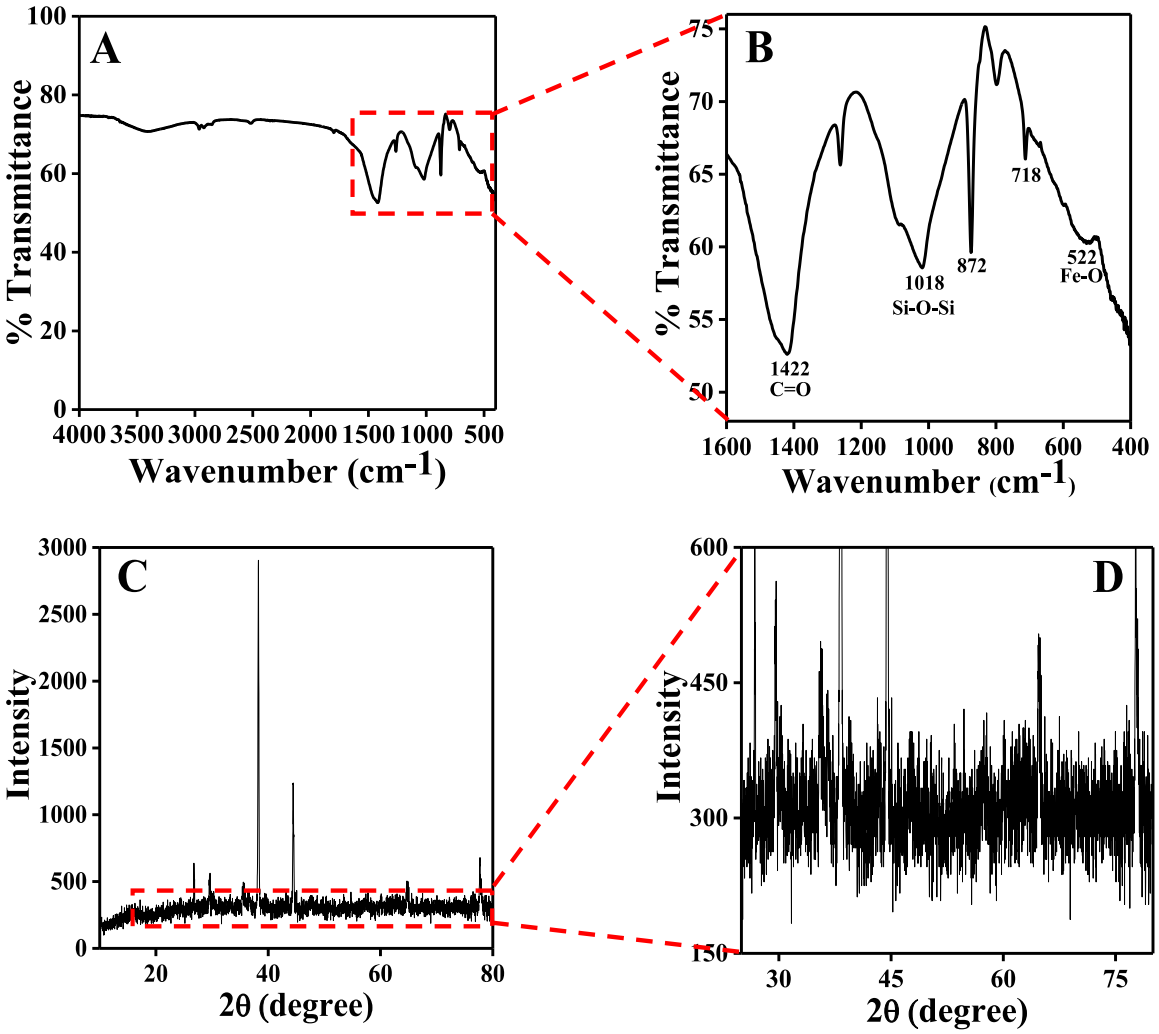

Fig. 8. FT-IR spectrum (A) Full spectrum at the range between 4000 and 400 cm^{-1}. (B) Enlarged spectrum of the same at the range of 1600–400 cm^{-1}. Powder-X-ray diffraction spectrum (C) Full-range diffractogram at the range between 10 and 80° (D) Enlarged diffractogram of the recovered Fe-NMs from ISA waste.

Table 3
Chemical composition of ISA analysed by XRF.

Elements	SiO_2	Al_2O_3	CaO	Fe_2O_3	MgO	K_2O	P_2O_5
Weight %	20.36	4.77	49.6	4.28	3.9	8.24	3.94

are formed due to the hematite and calcite phases in the ferrous particle samples (Dwivedi et al., 2012; Ilic et al., 2003; Sarkar et al., 2012). There are two small intensity peaks at 35.59° and 36.49°, due to the magnetite phases in the Fe-NMs. There is a reflection peak of magnetite at 77.5°. Additionally, there are two intermediate intensity peaks at 26.85° and 29.56° due to the quartz form and amorphous silica associated with the ferrous iron particles. Besides this, no other peaks were observed in the XRD spectrum.

The Fe^{2+}-NPs/Fe-NMs come from the coal powder, which constitutes 5%–8% of ISA. ISA contains around 50% calcium oxides by weight as confirmed by the analysis by XRF. Since it is ferrous iron, the alumina, silica, and Ca are present in the form of a complex mixture of calcium–ferro–aluminosilicate similar to coal fly ash. The average composition of calcium, silica, and ferrous iron material in the ISA is around 75%–77%. The total composition of the calcium–ferro–aluminosilicate complex is ∼80%, of which ferrous iron, alumina, silica, and calcium oxides are approximately 4.28%, 4.77%, 20.36%, and 49.6%, respectively, which was confirmed by the XRF analysis. Besides this, oxides of Mg, K, and P are also present, and their weight percentages are given in Table 3.

3.5. Practical applicability and future applications

The recovered ferrous fraction is impure due to the presence of trace elements, which is why it has to be further processed for the synthesis of highly pure ferrous particles. The recovered ferrous fraction could be directly used in nanoceramics (Fan and Kotov, 2020), as heterogeneous catalysts in petroleum industries, and for metallurgy purposes like in coke in steel manufacturing industries. Besides, it could be applied as an adsorbent for the remediation of wastewater treatment (Mushtaq et al., 2019; Prasad et al., 2021). A basic advantage of the ferrous particle is that it could be easily manipulated by an external magnetic field, which is why it could be recovered and reused after the completion of the experiment. It will act as an alternative source of ferrous materials and minimize the burden on the current iron-based industries.

4. Conclusions

Although incense sticks represent the most widely used material, the ashes generated from them do not have scientific applications. It has been one of the most overlooked by-products generated at temples and homes, especially in South-East Asian countries. High content of calcium, carbon, silica, alumina, and ferrous oxides has drawn the attention of ISA for recycling. The wet magnetic separation method was found efficient, recovering 15%–25% ferrous from ISA. The presence of quartz and calcium oxides by FTIR has confirmed the transformation of organic contents from coal powder used in ISA. The low temperature during incense sticks combustion favoured irregular to the spherical shape of ferrous, as confirmed by microscopy. Microscopy and DLS also confirmed the aggregation of numerous 20-nm ferrous particles to form large particles. The association of Fe with C, Si, Mn, Mg, Ca, Na, and Ti indicates the impurities which come from the coal powder. The high carbon in the ISA indicates unburnt carbon due to burning at low temperatures. The high carbon content and impurities can make a potential candidate for the recovery of carbon or fuel and heterocatalyst in petroleum industries. The current approach has suggested an alternative source of ferrous material for the industries, using economical and eco-friendly resource material.

Abbreviations

Fe-NMs: Iron nanominerals, XRD: X-ray diffraction, FTIR: Fourier's transform infrared spectroscopy, ISA: Incense stick ash, EDS: Energy-dispersive X-ray spectroscopy, FESEM: Field emission scanning electron microscope, TEM: Transmission electron microscope, XRF: X-ray Fluorescence.

Funding

This research was funded by [Taif University, Researchers Supporting Project] grant number [TURSP-2020/196].

CRediT authorship contribution statement

Nitin Gupta: Methodology, Writing – original draft, Writing – Review, Editing. **Virendra Kumar Yadav:** Supervision, Conceptualization, Methodology, Writing – original draft, Editing. **Krishna Kumar Yadav:** Supervision, Formal analysis, Writing – original draft, Writing – review & editing. **Mamdooh Alwetaishi:** Project administration, Data curation, Writing – original draft, Writing – review & editing. **G. Gnanamoorthy:** Formal analysis, Validation, Writing – review & editing. **Bijendra Singh:** Formal analysis, Validation, Writing – original draft. **Byong-Hun Jeon:** Resources, Writing – review & editing, Validation, Visualization. **Marina M.S. Cabral-Pinto:** Data curation, Writing – original draft, Visualization, Project administration. **Nisha Choudhary:** Formal analysis, Data curation, Writing – review & editing. **Daoud Ali:** Formal analysis, Writing – review & editing. **Zahra Derakhshan Nejad:** Formal analysis, Validation, Resources, Visualization.

Declaration of competing interest

The authors declare that they have no known competing financial interests or personal relationships that could have appeared to influence the work reported in this paper.

Acknowledgements

Authors would like to acknowledge the finical support provided from Taif University, Saudi Arabia Researchers Supporting Project Number (TURSP-2020/196). Funding for this research was (partially) provided by the Projects SFRH/BPD/71030/2010, Project UID/GEO/04035/2019 (geobiotec Research Centre) financed by FCT – Fundação para a Ciência e Tecnologia, Portugal.

References

Al-Ghouti, M.A., Khan, M., Nasser, M.S., Saad, K.A., Heng, O.E., 2020. Recent advances and applications of municipal solid wastes bottom and fly ashes: Insights into sustainable management and conservation of resources. Environ. Technol. Innov. 21, 101267. http://dx.doi.org/10.1016/j.eti.2020.101267.

Alavi, M.A., Morsali, A., 2010. Syntheses and characterization of $Sr(OH)_2$ and SrCO3 nanostructures by ultrasonic method. Ultrason. Sonochem. 17, 132–138. http://dx.doi.org/10.1016/j.ultsonch.2009.05.004.

Ali, H., Khan, E., Ilahi, I., 2019. Environmental chemistry and ecotoxicology of hazardous heavy metals: Environmental persistence, toxicity, and bioaccumulation. J. Chem. 2019, 6730305. http://dx.doi.org/10.1155/2019/6730305.

Bedini, S., 1963. The scent of time. a study of the use of fire and incense for time measurement in oriental countries. Trans. Am. Philos. Soc. 1–51. http://dx.doi.org/10.2307/1005923.

Biradar, S., Ravichandran, P., Gopikrishnan, R., Goornavar, V., Hall, J.C., Ramesh, V., Baluchamy, S., Jeffers, R.B., Ramesh, G.T., 2011. Calcium carbonate nanoparticles: Synthesis, characterization and biocompatibility. J. Nanosci. Nanotechnol. 11, 6868–6874. http://dx.doi.org/10.1166/jnn.2011.4251.

Cabral-Pinto, M.M.S., Inácio, M., Neves, O., Almeida, A.A., Pinto, E., Oliveiros, B., Ferreira da Silva, E.A., 2020. Human health risk assessment due to agricultural activities and crop consumption in the surroundings of an industrial area. Expo Health 12, 629–640. http://dx.doi.org/10.1007/s12403-019-00323-x.

Cui, W., Meng, Q., Feng, Q., Zhou, L., Cui, Y., Li, W., 2019. Occurrence and release of cadmium, chromium, and lead from stone coal combustion. Int. J. Coal Sci. Technol. 6, 586–594. http://dx.doi.org/10.1007/s40789-019-00281-4.

Dwivedi, S., Saquib, Q., Al-Khedhairy, A.A., Ali, A.Y.S., Musarrat, J., 2012. Characterization of coal fly ash nanoparticles and induced oxidative DNA damage in human peripheral blood mononuclear cells. Sci. Total Environ. 437, 331–338. http://dx.doi.org/10.1016/j.scitotenv.2012.08.004.

Elsayed, Y., Dalibalta, S., Gomes, I., Fernandes, N., Alqtaishat, F., 2016. Chemical composition and potential health risks of raw Arabian incense (Bakhour). J. Saudi Chem. Soc. 20, 465–473. http://dx.doi.org/10.1016/j.jscs.2014.10.005.

Ezhumalai, R., Kumar, R., Bisht, S.S., 2021. Analysis of gaseous pollutants during burning of natural and market based sandalwood oil incense stick. Int. J. Recent Sci. Res. 12, 40656–40658. http://dx.doi.org/10.24327/ijrsr.

Fan, J., Kotov, N.A., 2020. Chiral nanoceramics. Adv. Mater. 32, http://dx.doi.org/10.1002/adma.201906738.

Frans va, D., 2009. Council of the European Union: Ash Utilisation - Draft for Technical Regulations (D6.3). Available online: https://ec.europa.eu/research/participants/documents/downloadPublic?documentIds=080166e5c82e4e2f&appId=PPGMS.

Gombart, A.F., Pierre, A., Maggini, S., 2020. A review of micronutrients and the immune system–working in harmony to reduce the risk of infection. Nutrients 12 (236), http://dx.doi.org/10.3390/nu12010236.

Gupta, N., Yadav, K.K., Kumar, V., Kumar, S., Chadd, R.P., Kumar, A., 2019. Trace elements in soil-vegetables interface: translocation, bioaccumulation, toxicity and amelioration - A review. Sci. Total Environ. 651, 2927–2942. http://dx.doi.org/10.1016/j.scitotenv.2018.10.047.

Gupta, A., Yan, D.S., 2016. Magnetic and electrostatic separation, in mineral processing sesign and operations. In: Mineral Processing Design and Operations, second ed. Elsevier, Amsterdam, pp. 629–687. http://dx.doi.org/10.1016/b978-0-444-63589-1.00017-4.

Hanumappa, H.G., 1996. Agarbathi: A Bamboo-Based Industry in India. Institute of Social and Economic Change, International Development Research Centre, Bangalore, India, https://www.inbar.int/wp-content/uploads/2020/05/1489477022.pdf.

Hazarika, P., Dutta, N.B., Biswas, S.C., Dutta, R.C., Jayaraj, R.S.C., 2018. Status of agarbatti industry in India with special reference to Northeast. Int. J. Adv. Res. Biol. Sci. 5, 173–186.

Ilic, M., Cheeseman, C., Sollars, C., Knight, J., 2003. Mineralogy and microstructure of sintered lignite coal fly ash. Fuel 82, 331–336. http://dx.doi.org/10.1016/S0016-2361(02)00272-7.

Jain, S.N., Tamboli, S.R., Sutar, D.S., Mawal, V.N., Shaikh, A.A., Prajapati, A.A., 2020. Incense stick ash as a novel and sustainable adsorbent for sequestration of Victoria Blue from aqueous phase. Sustain. Chem. Pharm. 15, 100199. http://dx.doi.org/10.1016/j.scp.2019.100199.

Jetter, J.J., Guo, Z., McBrian, J.A., Flynn, M.R., 2002. Characterization of emissions from burning incense. Sci. Total Environ. 295, 51–67. http://dx.doi.org/10.1016/s0048-9697(02)00043-8.

Jilla, A., Kura, B., 2017. Particulate matter and carbon monoxide emission factors from incense burning. Environ. Pollut. Clim. Change 1, 4. http://dx.doi.org/10.4172/2573-458X.1000140.

Kanchan, S., Kumar, V., Yadav, K.K., Gupta, N., Arya, S., 2015. Effect of fly ash disposal on ground water quality near Parichha thermal power plant, Jhansi: A case study. Curr. World Environ. 30, 572–580. http://dx.doi.org/10.12944/cwe.10.2.21.

Kao, M.C., Wang, C.S., 2002. Reactive oxygen species in incense sticks. Aerosol Air Qual. Res. 2, 61–69. http://dx.doi.org/10.4209/aaqr.2002.06.0007.

Khale, D., Chaudhary, R., 2007. Mechanism of geopolymerization and factors influencing its development: A review. J. Mater. Sci. 42, 729–746. http://dx.doi.org/10.1007/s10853-006-0401-4.

Khan, S., Akhtar, N., Rehman, S.U., Shujah, S., Rha, E.S., Jamil, M., 2021. Biosynthesized iron oxide nanoparticles (Fe_3O_4 NPs) mitigate arsenic toxicity in rice seedlings. Toxics 9 (2), http://dx.doi.org/10.3390/toxics9010002.

Khezri, B., Chan, Y.Y., Tiong, L.Y.D., Webster, R.D., 2015. Annual air pollution caused by the Hungry Ghost Festival. Environ. Sci.: Process. Impacts 17, 1578–1586. http://dx.doi.org/10.1039/C5EM00312A.

Kumar, A., 2017. Agarbatti-The Sweet Scent of Profits. The Dollar Business, https://www.thedollarbusiness.com/magazine/agarbattithe-sweet-scent-of-profits/45966.

Li, G., Li, Z., Ma, H., 2013. Synthesis of aragonite by carbonization from dolomite without any additives. Int. J. Miner. Process. 123, 25–31. http://dx.doi.org/10.1016/j.minpro.2013.03.006.

Li, Y.J., Yeung, J.W.T., Leung, T.P.I., Lau, A.P.S., Chan, C.K., 2012. Characterization of organic particles from incense burning using an aerodyne high-resolution time-of-flight aerosol mass spectrometer. Aerosol Sci. Technol. 46, 654–665. http://dx.doi.org/10.1080/02786826.2011.653017.

Lin, T.C., Krishnaswamy, G., Chi, D.S., 2008. Incense smoke: Clinical, structural and molecular effects on airway disease. Clin. Mol. Allergy 6, 3. http://dx.doi.org/10.1186/1476-7961-6-3.

Lin, T.C., Yang, C.R., Chang, F.H., 2007. Burning characteristics and emission products related to metallic content in incense. J. Hazard. Mater. 140, 165–172. http://dx.doi.org/10.1016/j.jhazmat.2006.06.052.

Malav, L.C., Yadav, K.K., Gupta, N., Kumar, S., Sharma, G.K., Krishnan, S., Rezania, S., Kamyab, H., Pham, Q.B., Yadav, S., Bhattacharyya, S., Yadav, V.K., Bach, Q.V., 2019. A review on municipal solid waste as a renewable source for waste-to energy project in India: Current practices, challenges, and future opportunities. J. Cleaner Prod. 277, 123227. http://dx.doi.org/10.1016/j.jclepro.2020.123227.

Montoya-Bautista, C.V., Avella, E., Ramírez-Zamora, R.M., Schouwenaars, R., 2019. Metallurgical wastes employed as catalysts and photocatalysts for water treatment: A review. Sustain 11, 1–16. http://dx.doi.org/10.3390/su11092470.

Mukunda, H.S., Basani, J., Shravan, H.M., Philip, B., 2007. Smoldering combustion of incense sticks - Experiments and modeling. Combust. Sci. Technol. 179, 1113–1129. http://dx.doi.org/10.1080/00102200600970019.

Mushtaq, F., Zahid, M., Bhatti, I.A., Nasir, S., Hussain, T., 2019. Possible applications of coal fly ash in wastewater treatment. J. Environ. Manag. 240, 27–46. http://dx.doi.org/10.1016/j.jenvman.2019.03.054.

Prasad, S., Yadav, K.K., Kumar, S., Gupta, N., Cabral-Pinto, M.M.S., Rezania, S., Radwan, N., Alam, J., 2021. Chromium contamination and effect on environmental health and its remediation: A sustainable approaches. J. Environ. Manag. 285, 112174. http://dx.doi.org/10.1016/j.jenvman.2021.112174.

Quina, M.J., Bontempi, E., Bogush, A., Schlumberger, S., Weibel, G., Braga, R., Funari, W., Hyks, J., Rasmussen, E., Lederer, J., 2018. Technologies for the management of MSW incineration ashes from gas cleaning: New perspectives on recovery of secondary raw materials and circular economy. Sci. Total Environ. 635, 526–542. http://dx.doi.org/10.1016/j.scitotenv.2018.04.150.

Ramya, H.G., Palanimuthu, V., Dayanandakumar, R., 2003. Patchouli in fragrances-incense stick production from patchouli spent charge powder. Agric. Eng. Int: CIGR J. 15, 187–193.

Saha, S., Reza, A.H.M.S., Roy, M.K., 2019. Hydrochemical evaluation of groundwater quality of the Tista floodplain, Rangpur, Bangladesh. Appl. Water Sci. 9, 198. http://dx.doi.org/10.1007/s13201-019-1085-7.

Salavati-Niasari, M., Sabet, M., Fard, Z.A., Saberyan, K., Hosseinpour-Mashkani, S.M., 2015. Synthesis and characterization of calcium carbonate nanostructures via a simple hydrothermal method. Synth. React. Inorg. Met. Nano-Metal Chem. 45, 848–857. http://dx.doi.org/10.1080/15533174.2013.862643.

Sarkar, A., Vishwakarma, S., Banichul, H., Mishra, K.K., Roy, S.S., 2012. A comprehensive analysis of the particle size and shape of fly ash from different fields of ESP of a super thermal power plant. Energy Source A 34, 385–395. http://dx.doi.org/10.1080/15567031003614649.

See, S.W., Balasubramanian, R., 2011. Characterization of fine particle emissions from incense burning. Build. Environ. 46, 1074–1080. http://dx.doi.org/10.1016/j.buildenv.2010.11.006.

Sibiya, N.P., Rathilal, S., Tetteh, E.K., 2021. Coagulation treatment of wastewater: Kinetics and natural coagulant evaluation. Molecules 26 (698), http://dx.doi.org/10.3390/molecules26030698.

Smołka-Danielowska, D., Kądziołka-Gaweł, M., Krzykawski, T., 2019. Chemical and mineral composition of furnace slags produced in the combustion process of hard coal. Int. J. Environ. Sci. Technol. 16, 5387–5396. http://dx.doi.org/10.1007/s13762-018-2122-z.

Tavker, N., Yadav, V.K., Yadav, K.K., Cabral-Pinto, M.M., Alam, J., Shukla, A.K., Ali, F.A.A., Alhoshan, M., 2021. Removal of cadmium and chromium by mixture of silver nanoparticles and nano-fibrillated cellulose isolated from waste peels of citrus sinensis. Polymers 13 (234), http://dx.doi.org/10.3390/polym13020234.

Tetteh, E.K., Rathilal, S., 2020. Application of Organic Coagulants in Water and Wastewater Treatment. Intech Open, http://dx.doi.org/10.5772/intechopen.84556.

Valeev, D., Kunilova, I., Alpatov, A., Varnavskaya, A., Ju, D., 2019. Magnetite and carbon extraction from coal fly ash using magnetic separation and flotation methods. Minerals 9 (350), http://dx.doi.org/10.3390/min9050320.

Vardhan, K.H., Kumar, P.S., Panda, R.C., 2019. A review on heavy metal pollution, toxicity and remedial measures: Current trends and future perspectives. J. Mol. Liq. 290, 111197. http://dx.doi.org/10.1016/j.molliq.2019.111197.

Venkateswarlu, V., Venkatrayulu, C., 2020. Bioaccumulation of heavy metal lead (Pb) in different tissues of brackish water fish Mugil cephalus (Linnaeus, 1758). J. Appl. Biol. Biotechnol. 8, 1–5. http://dx.doi.org/10.7324/JABB.2020.80201.

Yadav, V.K., Gnanamoorthy, G., Cabral-Pinto, M.M.S., Alam, J., Ahamed, M., Gupta, N., Yadav, K.K., 2021. Variations and similarities in structural, chemical, and elemental properties on the ashes derived from the coal due to their combustion in open and controlled manner. Environ. Sci. Pollut. Res. 1–17. http://dx.doi.org/10.1007/s11356-021-12989-5.

Yadav, V.K., Yadav, K.K., Gnanamoorthy, G., Choudhary, N., Khan, S.H., Gupta, N., Bach, Q.V., 2020. A novel synthesis and characterization of polyhedral shaped amorphous iron oxide nanoparticles from incense sticks ash waste. Environ. Technol. Innov. 20, 101089. http://dx.doi.org/10.1016/j.eti.2020.101089.

Yang, C.R., Lin, T.C., Chang, F.H., 2006. Correlation between calcium carbonate content and emission characteristics of incense. J. Air Waste Manage. Assoc. 56, 1726–1732. http://dx.doi.org/10.1080/10473289.2006.10464577.

Yeh, K., Song, Z., Reznichenko, J., Jang, K.O., 1993. Alkali metal ions and their effects on smoldering and ignition of cotton upholstery fabrics- A literature review. J. Fire Sci. 11, 350–354. http://dx.doi.org/10.1177/073490419301100406.

Zarenezhad, M., Zarei, M., Ebratkhahan, M., Hosseinzadeh, M., 2021. Synthesis and study of functionalized magnetic graphene oxide for Pb^{2+} removal from wastewater. Environ. Technol. Innov. 22, 101384. http://dx.doi.org/10.1016/j.eti.2021.101384.

Zierold, K.M., Sears, C.G., Hagemeyer, A.N., Brock, G.N., 2020. Protocol for measuring indoor exposure to coal fly ash and heavy metals, and neurobehavioural symptoms in children aged 6 to 14 years old. BMJ Open 10, e038960. http://dx.doi.org/10.1136/bmjopen-2020-038960.